Investigating the Effect of High Power Diode Laser (HPDL) Surface Treatment on the Corrosion Behavior of 17-4 PH Martensitic Stainless Steel

Moradi, M., Karami Moghadam, M., Fallah, M. M. & Hesadi, M.

Original citation & hyperlink:
Moradi, M, Karami Moghadam, M, Fallah, MM & Hesadi, M 2020, 'Investigating the Effect of High Power Diode Laser (HPDL) Surface Treatment on the Corrosion Behavior of 17-4 PH Martensitic Stainless Steel', Lasers in Engineering, vol. 46, no. 1-4, pp. 245-256.

https://www.oldcitypublishing.com/journals/lie-home/lie-issue-contents/lie-volume-46-number-1-4-2020/lie-46-1-4-p-245-156/

ISSN 0898-1507
ESSN 1029-029X

Publisher: Old City Publishing

Investigating the Effect of High Power Diode Laser Surface Treatment on the Corrosion Behavior of 17-4 PH Martensitic Stainless Steel

Mahmoud Moradi[1, 2, *], Mojtaba Karami Moghadam[1, 2], Mohammad Meghdad Fallah[3], Miad Hesadi[4]

[1]Department of Mechanical Engineering, Faculty of Engineering, Malayer University, P.O.B. 65719-95863, Malayer, Iran

[2]Laser Materials Processing Research Center, Malayer University, Malayer, Iran

[3]Shahid Rajaee Teacher Training University, Lavizan, Tehran, Iran, P. O. Box: 16785-163.

[4]Technical and Vocational Training Organization, Kermanshah, Iran

[*]*Corresponding author:* moradi@malayeru.ac.ir

ABSTRACT

In the present work, the laser surface treatment conducted using a High Power Diode Laser (HPDL) to improve the corrosion resistance of 17-4 PH stainless steel. Based on microstructure and corrosion behavior study, stand of distance (SOD) (60-80mm), laser power (1000-1400 W) and scanning speed (5-8 mm/s) were considered as process parameters. The Martensite formed in this alloy is of a lath morphology having a dislocated substructure. Microscopy studies have revealed the formation of a copper-rich phase in the samples aged at temperatures below 550 °C. The martensite phase was seen to terminate at packet boundaries where two groups of laths belonging to two distinct orientation variants met. Corrosion tests using IVIUMSTAT apparatus in 3.5 wt% NaCl solution. After HPDL treatment, the corrosion resistance of 17Cr4Ni PH steel has not improved.

Keyword**:** High Power Diode Laser; 17-4 PH Steel; Micro-hardness; Microstructure; Corrosion.

1. INTRODUCTION

Laser technology is extensively applied to improving manufacturing processes [1-3]. Recently, laser materials processing was very important in the many of industrial field. Such as in forming, welding, cutting, hardening, and etc. [4-11]. 17-4 PH Martensitic Stainless Steel is one of the most familiar industrial steels. It is used in vessels, pipes, and exterior shell of the many tools due to its corrosion and wear resistance. In the literature, there are several works on laser source used in manufacturing processes such as laser welding, laser cutting, and laser hardening, Laser drilling, Laser engraving, laser additive manufacturing and etc [12-17]. Laser surface treatment is a promising process for enhancing the surface properties of ferrous products. In this process, a moving laser beam heat treats the part surface layer and could increase the corrosion resistance while remaining the base material unaffected. This method has some advantages relative to conventional methods regarding the effectiveness and accuracy of the process [18].

Martensitic stainless steel has proper mechanical properties and extremely used in both high and low-temperature condition including gas and steam turbine and vessels industries. Martensite is an expedient hard phase which is sufficient for surfaces exposed to wear and corrosion. In laser surface treatment of martensitic parts, the workpiece surface warms up to austenite temperature, and after cooling process, the Martensite phase will construct in the surface. This process usually use for enhancing mechanical behavior and wear and corrosion resistance of martensitic parts.

Aiming et al. [19] studied the material AISI 410 under simultaneous wear and corrosion condition and attempted to improve it via several surface treatment processes. Mahmoudi et al. [20] work on surface hardening of AISI 410 martensitic stainless steel by pulsed solid-state Nd:YAG laser with a maximum power of 400 W. In their work, the process parameters optimized for enhancing the surface hardness and corrosion behavior. Numerical and experimental analysis of the Nd:YAG laser surface hardening with overlapped tracks for designing AISI 410 process considering different criteria was done by Cordovilla et al. [21]. Krishna et al. [22] studied the fatigue properties of laser engineered net-shaped AISI 410. The microstructure of melted surfaces depends on process parameters, and they found that an increase in the amount of retained austenite will reduce the final hardness. Also, retained austenite is one of the most critical factors affecting the corrosion behavior of martensitic steels. Zirepour et al. [23] optimized the Nd:YAG laser local hardening process of AISI 420 regarding the wear properties of turbine blades. According to their work, this process leads to martensitic-austenitic microstructure in the surface. Another work on AISI 420 performed by Mahmoudi et al. [24] for obtaining the optimum hardness using Nd:YAG laser process. In their work, the effect of laser pulse energy, duration time, and travel speed on hardened depth were investigated. Jahromi et al. [25] investigated the effect of laser surface treatment process on different microstructure of AISI 420 achieved by various pre-heat treatments. Their results revealed the effectiveness of the process on all microstructures. Al-Sayed et al. [26] examined the wear and corrosion behavior of hardened AISI 416 under different Nd:YAG laser powers and scanning speeds and compared the results with the conventional process. They showed that the corrosion behavior of AISI 416 is related to samples carbides, magnesium sulfide impurities in grain boundaries and microstructure. For other steels, Nd:YAG laser surface hardening with different inputs applied for studying microstructure, residual stress and mechanical properties of austempered ductile iron grades [27], microstructure of low carbon steels after hardening process [28], the effect of laser scanning speed on laser hardening of AISI 440C [29], hardening of low alloy steel EN25 to achieve optimized parameters to increase hardness [30] and laser hardening of tools steels and perform wear test on them [31]. For unalloyed titanium, Badkar et al. [32] used response surface methodology for the empirical study of Nd:YAG laser hardening process. They statistically calculated the geometrical dimensions of the affected area and found that by reducing laser scanning speed and increasing laser power, the dimensions of hardened areas increases. 17-4 PH is a martensitic precipitation-hardening stainless steel frequently used in industry due to its high strength, excellent corrosion resistance, and mechanical properties at relatively high temperatures. Tsay et al. [33] worked on laser surface annealing treatment of 17-4 PH stainless steel. In their work, stress corrosion cracking and fatigue crack growth behavior was studied under various metallurgical conditions.

In this work, high power diode laser (HPDL) surface treatment was studied for enhancing the corrosion resistance of 17-4 PH surface. The process variables parameters were SOD (60-80mm), scanning speed (5-8 mm/s) and Laser Power (1000-1400 W). The effect of the process on microstructure and micro-hardness of samples were investigated.

2. EXPERIMENTS

The chemical composition of 17-4 PH material used in the experiment measured by Quantometer (ARL-3460) at temperature 23°C and moisture content 33% shown in Table 1.

TABLE 1 Chemical composition of 17-4 PH (weight %)

C	Si	S	P	Mn	Ni	Cr	Mo	Cu	Al	Ti	Sn	V
0.07	0.19	0.001	0.026	0.45	4.52	16.28	0.14	3.59	0.045	0.014	0.27	0.040

A diode continuous-wave (CW) laser with a maximum power of 1600 W and wavelength 808 nm was used in the experiments. The scanning speed (5-8 mm/s), SOD (60-80mm), and the laser power (1000-1400 W) were considered as independent input variables. The corrosion behavior of processed sample assessed using an IVIUMSTAT apparatus in 3.5 wt% NaCl solution. The Schematic of the laser surface treatment process and corrosion tests are shown in Figure 1. Also, Figure 2 shows the process set up of Nd:YAG laser treatment and corrosion tests for 17-4PH steel. Figure 3 shows the laser surface treated portion of a sample. After the process, the samples were sectioned and mounted for studying the cross-section, and the microhardness profile was measured using a micro-indentation device (BUEHLER, MH-73-01) in the laser penetration area. The microhardness measured using a maximum load of 100 gr and a dwell time 30 s. Figure 4 shows Vickers indenters in depth and width of the hardened area. For metallographic investigations, the hardened cut specimens polished and etched in the villa's reagent, ($C_6H_3N_3O_7$ 2gr, Hcl 5cc, C_2H_5OH 100cc). Also, an optical microscopy Leica MEF 4A with 50-100X magnification used for microstructure analysis.

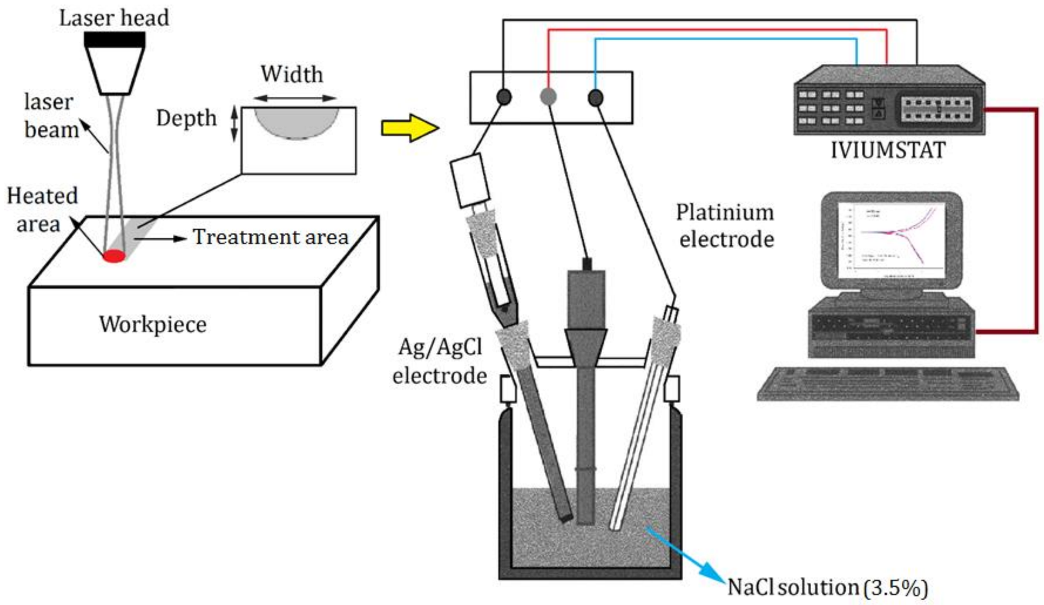

FIGURE 1 Schematic of treatment process and corrosion tests [34]

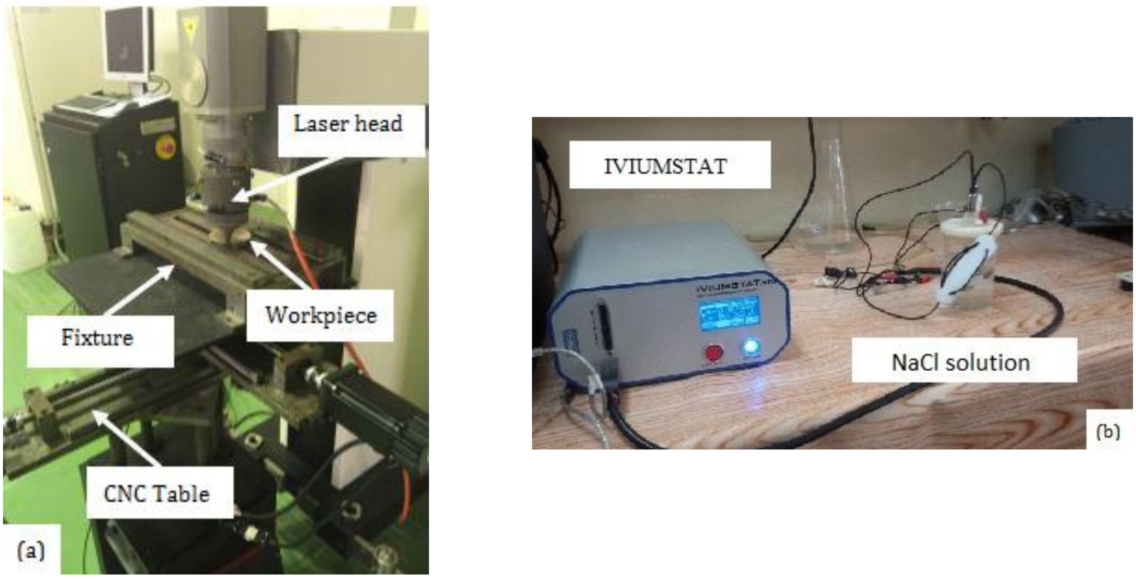

FIGURE 2 The process set up a) Nd:YAG Laser treatment b) corrosion tests

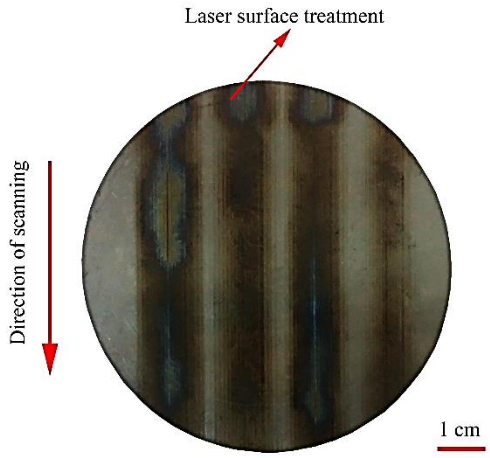

FIGURE 3 Laser surface the treatment of a sample

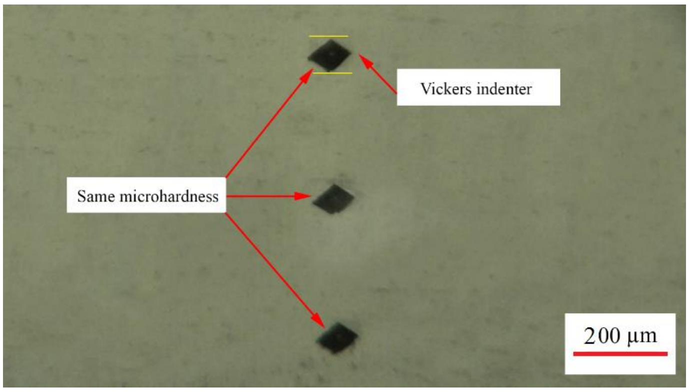

FIGURE 4 Cross-section of Vickers indenters in depth of treatment area

3 RESULTS AND DISCUSSION

For each process condition, the distribution of microhardness in the depth and width of the treated area measured and plotted. Also, the microstructure of the samples section observed using optical microscopy, and corrosion behavior of laser treatment samples was analyzed.

3.1 MICRO-HARDNESS AND MICROSTRUCTURE

Table 2 shows the parameters set in the experiments besides the relevant microhardness of processed samples, which were measured 50 micrometers below the surface at the track center. The experiments in this article are designed to estimate the impact of each parameters on laser surface treatment during the operation. It is worth noting that many experiments have been carried out on the Laser speed, Laser power and SOD, but the best of them are reported in this article.

TABLE 2 Experimental layout and multi-performance results

Experiment No.	Input variables			Microhardness (HV)
	Speed [mm/s]	Laser power [W]	SOD [mm]	
1	5	1400	65	227
2	8	1200	70	222
3	6	1200	70	225
4	6	1200	60	227
5	6	1200	80	223
6	7	1000	75	223
7	7	1000	65	227
8	5	1000	75	224
9	5	1000	65	227
10	7	1400	65	222

Figure 5 depicts the trend of microhardness changes along with the depth and width of sections for samples 3, 4, and 5. As shown, the micro-hardness of the processed areas has not significantly changed.

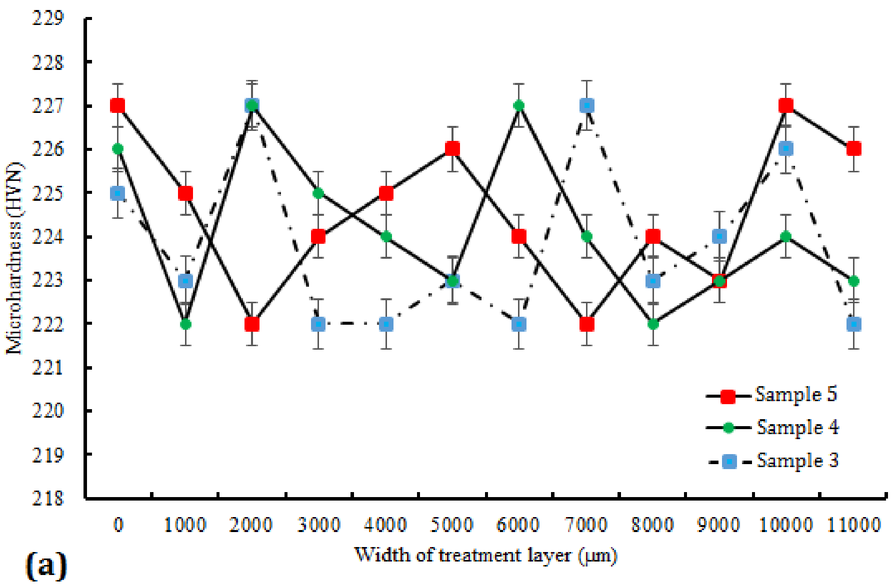

(a)

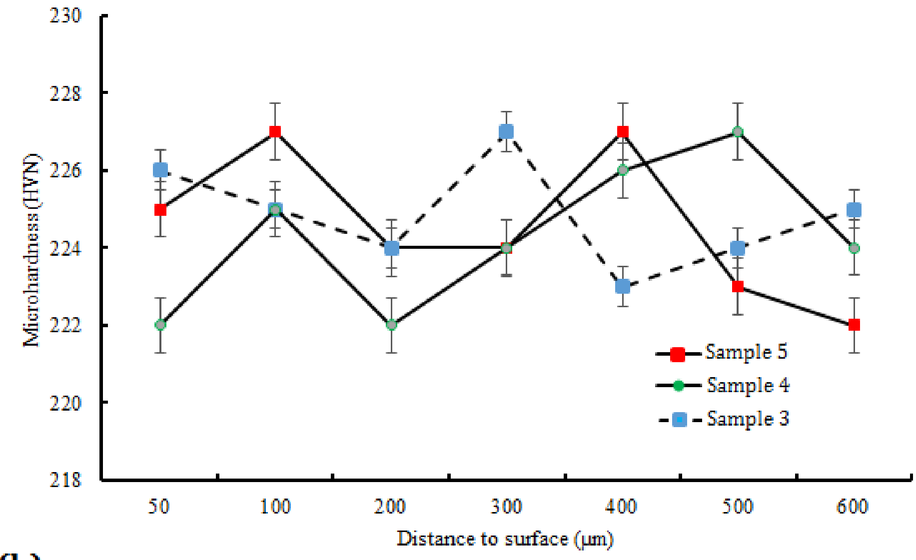

(b)

FIGURE 5 Micro-hardness distribution for samples #3, #4 and #5 a) along the width of samples b) along with the depth of samples

The transverse cross-section of the as-received rod show decreasing volume fractions of δ-ferrite and carbide precipitates from the center to the periphery. The Martensite formed in this alloy has been found to be of a laminar morphology having a dislocated substructure. Microscopy studies have revealed the formation of a copper-rich phase in the samples aged at temperatures below 550 °C (Figure 6-a). As shown in Figure 6-b, heat input has made a little change in the 17-4 PH structure.

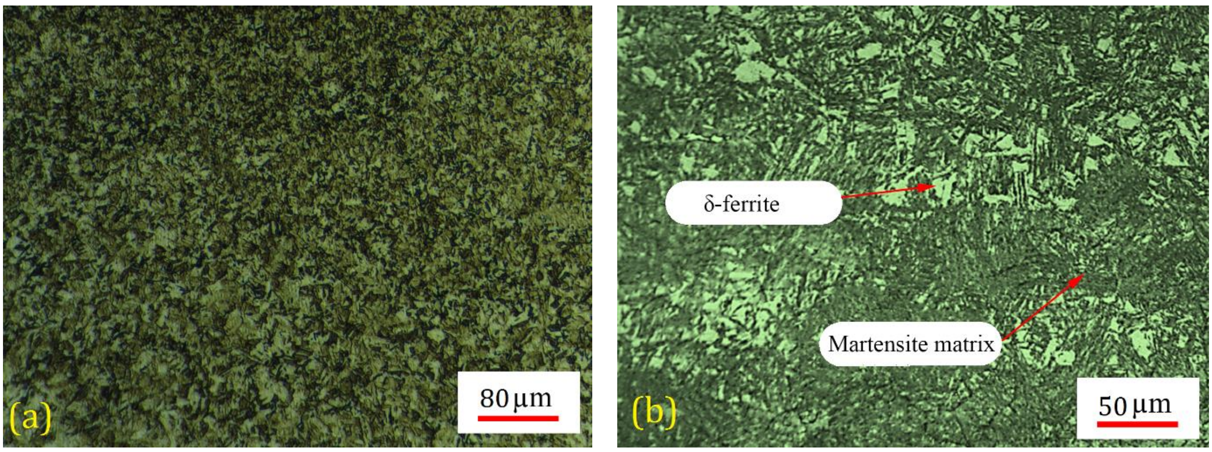

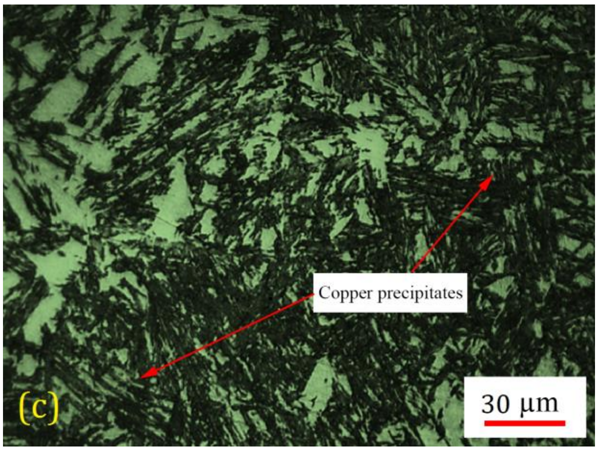

FIGURE 6 Microstructure of the laser treatment zone of sample #5 a) magnification 50 X from laser surface treatment b) Martensite and ferrite phases c) copper particles in the Martensite matrix

3-2 CORROSION

In some references [35-37] it is mentioned that corrosion behavior of 17-4 PH steels depends on two microstructural factors: a) amount and size of carbides and b) retained austenite. Carbides are rich in chromium in steels of high chromium content, because chromium has a high tendency for forming carbide. Increasing the carbides of structure leads to trapping more chromium in carbide phases and reducing the remained chromium for forming a passive layer, therefore the corrosion resistance decreases. Also, the carbides with bigger sizes made the microstructure more heterogeneous and so have a worse effect on material corrosion resistance. On the other side, due to the higher resistance of the austenite phase against corrosion rather than martensite, therefore retained austenite will improve corrosion resistance. Another factor that could improve surface corrosion resistance after laser hardening is cleaning the surface from undesirable impurities [38].

In potentiodynamic polarization tests, the potential plotted against current density, which respectively demonstrates the thermodynamic tendency for corroding phenomena. By decreasing the potential while increasing the current density, the thermodynamic tendencies to corrosion and corrosion rate will increases. This issue is shown in Figures 7.

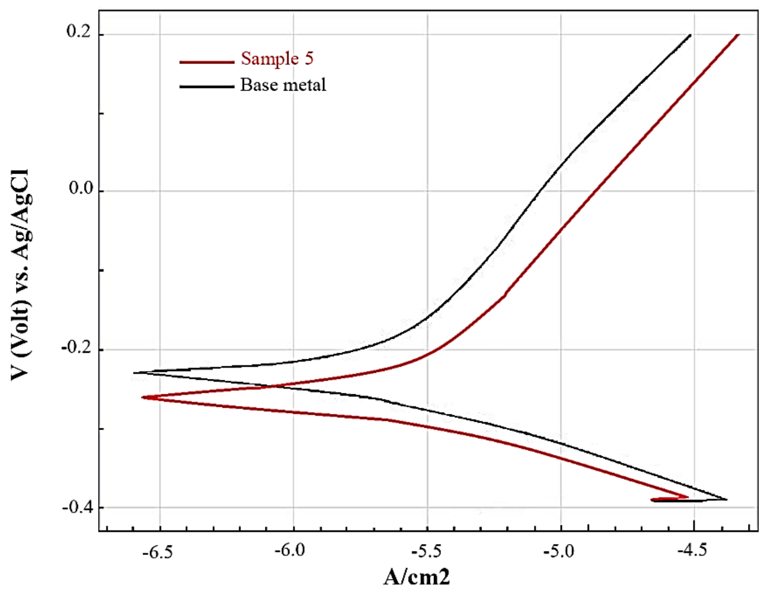

FIGURE 7 Comparative polarization diagram of samples #5 and base metal

The extracted current density of base metal and sample 5 from polarization curves are shown in Tables 4.

TABLE 4 Current density data for 17-4 PH samples

Samples	base	#1	#2	#3	#4	#5	#6
i_{corr}(A/cm^2)	6.52	6.83	6.95	6.81	6.9	6.6	6.72

The corrosion resistance in samples due to polarization test results was for sample #5. According to Figure 7 and Table 4 for this sample potential goes toward negative values, and current density decreases. Therefore, increasing laser heat input in sample #5 resulted in less retained austenite, lower hardness value, and lower resistance against corrosion. Also the Irregular austenite phase along to retained austenite in 17-4 PH steel after HPDL treatment, it reduces corrosion resistance.

4 CONCLUSION

In this research, the capability of laser surface treatment of AISI 17-4 PH steel was conducted using an HPDL. SOD, scanning speed, and Power laser were considered as laser input parameters, and also the micro-hardness of the hardened area was measured. Finally, the effects of parameters on corrosion behavior of hardened steel were studied. The micro-hardness of the hardened areas of samples by HPDL is changed irregular. This steel, after laser surface treatment for increasing the surface hardness, requires heating in the furnace, which creates the δ- ferrite phase to Martensite. Heat input of HPDL has made a little change in the 17-4 PH structure. Decreasing volume fractions of δ-ferrite and carbide precipitates from the center to the periphery. The martensite formed in this alloy has been found to be of a lath morphology having a dislocated substructure. Microscopy studies have revealed the formation of a copper-rich phase in the samples aged at temperatures below 550 °C. As potential goes toward fewer values and current density increases, the thermodynamic tendency to corrosion and corrosion rate will increase. The more corrosion resistance with a corrosion current density of 6.25 A/cm2 was obtained for the base metal. In sample 5, the corrosion current density of 6.6 A/cm2 was obtained. This shows that the corrosion resistance decreases.

REFERENCES:

[1] M. SafariM, M. FarzinM. (2015). Experimental investigation of laser forming of a saddle shape with spiral irradiating scheme, Optics & Laser Technology, 66,146-150.

[2] M. Safari, H. Mostaan, M. Farzin. (2016). Laser bending of tailor machined blanks: Effect of start point of scan path and irradiation direction relation to step of the blank, Alexandria Engineering Journal, 55 (2), 1587-1594.

[3] H. Mostaan, M. Shamanian, S. Hasani, M. Safari, J. A. Szpunar. (2017). Nd:YAG laser microwelding of ultra-thin FeCo–V magnetic alloy: optimization of weld strength, Transactions of Nonferrous Metals Society of China, 27 (8), 1735-1746.

[4] M. Safari, H. Mostaan. (2016). Experimental and numerical investigation of laser forming of cylindrical surfaces with arbitrary radius of curvature, Alexandria Engineering Journal, 55 (3), 1941-1949.

[5] M. Safari, M. Farzin, H. Mostaan. (2017). A novel method for laser forming of two-step bending of a dome shaped part, Iranian Journal of Materials Forming, 4 (2), 1-14.

[6] M. Safari, J. Joudaki. (2018). Prediction of Bending Angle for Laser Forming of Tailor Machined Blanks by Neural Network, Iranian Journal of Materials Forming, 5 (1), 47-57.

[7] M. Moradi, D. Ghorbani, M. K. Moghadam, M. Kazazi, F. Rouzbahani, S. Karazi, Nd:YAG laser hardening of AISI 410 stainless steel: Microstructural evaluation, mechanical properties, and corrosion behavior, Journal of Alloys and Compounds 795, 213-222.

[8] B. Martin, A. Loredo, D. Grevey, A.B. Vannes. (2001). Numerical investigation of laser beam shaping for heat transfer control in laser processing, Lasers in Engineering, 12 (4), 247-269.

[9] J. Lawrence, D. MacLellan. (2018). Industrial Laser Applications Symposium (ILAS 2017) Preface, Lasers in Engineering, 39 (1-2), 1-2.

[10] S. Nath, P. Shukla, XJ. SHEN, J. Lawrence. (2018). Effect of laser shock peening (LSP) on the phase evolution, residual stress and hardness of Hastelloy-X superalloys, Lasers in Engineering, 39 (1-2).

[11] J. Lawrence. (2017). Prelude to the International Journal of Laser Science: Fundamental Theory and Analytical Methods Preface, Lasers in Engineering, 38 (3-6), 125-126.

[12] M. Moradi, M. Ghoreishi, A. Khorram. (2018). Process and Outcome Comparison Between Laser, Tungsten Inert Gas (TIG) and Laser-TIG Hybrid Welding, Lasers in Engineering, 39 (3), 379-391.

[13] M. Moradi, A. Khorram, M. M. Fallah. (2019). Nd:YAG Laser Welding of Ti 6-Al-4V: Mechanical and Metallurgical Properties, Lasers in Engineering, 43 (1-3), 21-33.

[14] M Moradi, H Abdollahi. (2018). Statistical Modelling and Optimization of the Laser Percussion Microdrilling of Thin Sheet stainless Steel, Lasers in Engineering, 40 (4-6), 375-393.

[15] E Haddadi, M. Moradi, A. Karimzad Ghavidel, A. Karimzad Ghavidel. (2019). Experimental and Parametric Evaluation of Cut Quality Characteristics in CO_2 Laser Cutting of Polystyrene, Optik, 184, 103-114

[16] M. Moradi, M. Karami Moghadam, J. Zarei, B. Ganji. (2017). The effects of laser pulse energy and focal point position on laser surface hardening of AISI 410 stainless steel, Modares Mechanical Engineering 17 (6), 311-318.

[17] M. Moradi, M. karami moghadam. (2019). High Power Diode Laser Surface Hardening of AISI 4130; Statistical Modelling and Optimization, Optics and Laser Technology, 111, 554-570.

[18] Dowden J. (2009). The Theory of Laser Materials Processing: Heat and Mass Transfer in Modern Technology. Dordrecht: Springer Science, Business Media B.V.

[19] Aiming, F., L. Jinming, and T. Ziyun. (1996). An investigation of the corrosive wear of stainless steels in aqueous slurries. Wear, 1:193, 73-77.

[20] B. Mahmoudi, M.J Torkamany. (2010). Laser surface hardening of AISI 420 stainless steel treated by pulsed Nd:YAG laser. Materials & Design. 31(5), 2553-2560.

[21] F. Cordovilla, A. Garcia-Beltran, P. Sancho, J. Dominguez, L. Ruiz-de-Lara, J. L. Ocana. (2016), Numerical/experimental analysis of the laser surface hardening with overlapped tracks to design the configuration of the process for Cr-Mo steels. Materials & Design, 102, 225-237.

[22] Krishna, B.V, A. Bandyopadhyay. (2009). Surface modification of AISI 410 stainless steel using laser engineered net shaping (LENS TM). Materials & Design, 30:5, 1490-1496.

[23] Zirehpour, G., R. Shoja Razavi, E. Moayerifar. (2012). Evaluating Wear Properties of AISI 420 Martensitic Stainless Steel after Laser Transformation Hardening. International Journal of Iron & Steel Society of Iran, 9:2, 5-8.

[24] Mahmoudi, B., A.S. Aghdam, M. Torkamany. (2010). controlled laser transformation hardening of martensitic stainless steel by pulsed Nd:YAG laser. Journal of Electronic Science and Technology, 8:1, 87-90.

[25] Jahromi, S.J, A. Khajeh, and B. Mahmoudi. (2012). Effect of different pre-heat treatment processes on the hardness of AISI 410 martensitic stainless steels surface-treated using pulsed neodymium-doped yttrium aluminum garnet laser. Materials & Design, 34, 857-862.

[26] Al-Sayed, S. (2017). Characterization of a Laser Surface-Treated Martensitic Stainless Steel. Materials, 10:6, 595.

[27] Soriano, C. (2011). Effect of laser surface hardening on the microstructure, hardness and residual stresses of austempered ductile iron grades. Applied Surface Science, 257:16, 7101-7106.

[28] Jong-Do, K. (2009). Laser transformation hardening on rod-shaped carbon steel by Gaussian beam. Transactions of Nonferrous Metals Society of China, 19:4, 941-945.

[29] Lo, K., F. Cheng, H. Man. (2003). Laser transformation hardening of AISI 440C martensitic stainless steel for higher cavitation erosion resistance. Surface and Coatings Technology, 173:1, 96-104.

[30] Babu, P.D, G. Buvanashekaran, K.R. Balasubramanian. (2012). Experimental studies on the microstructure and hardness of laser transformation hardening of low alloy steel. Transactions of the Canadian Society for Mechanical Engineering. 36:3, 242-257.

[31] I. A. Pinahin, V. A. Chernigovskij, A. A. Bracihin, M. A. Yagmurov. (2015). Improvement of wear resistance of VK6, VK8, T5K10, and T15K6 hard alloys by volume pulsed laser hardening. Journal of Friction and Wear, 36:4, 330-333.

[32] Badkar, D, K. Pandey, G. Buvanashekaran. (2010), Effects of laser phase transformation hardening parameters on heat input and hardened-bead profile quality of unalloyed titanium. Transactions of Nonferrous Metals Society of China, 20:6, 1078-1091.

[33] L.W. Tsay, T.Y. Yang, M.C. Young (2001), Embrittlement of laser surface-annealed 17-4 PH stainless steel, Materials Science and Engineering: A, Volume 311, Issues 1–2: 64-73.

[34] M. Moradi, M. Karami Moghadam, M. Kazazi. (2019). Improved laser surface hardening of AISI 4130 low alloy steel with electrophoretically deposited carbon coating, Optik, 178, 614-622.

[35] Asm metals handbook. (1992). Metallography and microstructures, The materials information company, 9.

[36] C. W. Li, K. C. Chang, A. C. Yeh, J. W. Yeh, S. J. Lin. (2018). Microstructure characterization of cemented carbide fabricated by selective laser melting process, International Journal of Refractory Metals and Hard Materials, 75, 225-233.

[37] Y. Zhang, C. Ding, L. Pan, Y. Cai. (2018). Laser arrays of partially coherent beams with multi-Gaussian correlation function, Journal of Quantitative Spectroscopy and Radiative Transfer, 218, 1-11.

[38] Leonard R. Migliore. (1996). Manufacturing engineering and materials processing, Laser materials processing, Dekker, 46.